JOC The Journal of Organic Chemistry

Article

pubs.acs.org/joc

# Photochromic Molecular Gyroscope with Solid State Rotational States Determined by an Azobenzene Bridge

Patrick Commins and Miguel A. Garcia-Garibay*

Contribution from the Department of Chemistry and Biochemistry, University of California, Los Angeles, California 90095-1569, United States

Supporting Information

**ABSTRACT:** We describe the synthesis, characterization, photochemical isomerization, and rotational dynamics of a crystalline molecular gyroscope containing an azobenzene bridge (*trans*-**2**) that spans from one end of the stator to other, with the intention of exploring its function as a molecular brake. While single crystal X-ray diffraction analysis of a photochemically inactive dichloromethane solvate was used to confirm the molecular and packing structures of *trans*-**2**, a nanocrystalline pseudopolymorph was shown to be photoactive, and it was analyzed by powder X-ray diffraction (PXRD), scanning electron microscopy, and variable temperature solid state $^2$H NMR before and after photoisomerization. It was shown that the nanocrystalline suspension irradiated with $\lambda$ = 340 nm reaches a photostationary state with 34% of *cis*-isomer, as compared to that observed in solution where the corresponding value is 74%. Line shape analysis of solid state $^2$H NMR spectra of a phenylene-$d_4$ isotopologue, obtained as a function of temperature, indicated that rotation in crystals of the *trans*-**2** isomer, with a mean activation energy of 4.6 ± 0.6 kcal/mol and a pre-exponential factor exp(29.4 ± 1.7), is ten times faster than that of samples containing the *cis*-**2** isomer, which has a higher mean activation energy of 5.1 ± 0.6 kcal/mol and a lower pre-exponential factor of exp(27.9 ± 1.3).

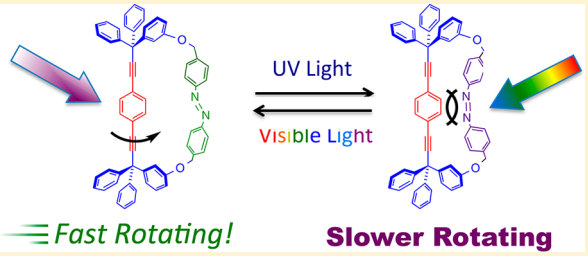


## INTRODUCTION

Interest in artificial molecular machines has driven chemists to explore the design and synthesis of molecules that can be switched from one state to another[1] with suitable external stimuli in order to display functions that take advantage of thermal oscillations. A few years ago we suggested that a promising platform for the design of artificial molecular machines might take the form of "amphidynamic crystals"[2] built with rigid components that sustain their lattice architecture and mobile components that explore fast, large amplitude motions, designed to perform specific functions. To realize a combination of fast motion and crystalline order, we decided to emulate and analyze the structure of macroscopic gyroscopes, which may form an ordered lattice while allowing for the fast motion of their internal rotator (Figure 1). To ensure rapid rotational dynamics, we selected a 1,4-substituted phenylene as the rotator and two alkynyl linkages as a nearly "barrierless" axle.[3] One approach toward accessing molecular frameworks with controllable molecular dynamics has been utilizing shielded or "bridged" molecular gyroscopes.[4] In our initial work, the rotator was shielded from intermolecular close contacts by a pair of bulky trityl groups acting as the stator. The installation of groups that bridge the structure from one trityl stator to the other in order to prevent interdigitation and provide better shielding to the rotator was met with partial success. While three benzophenone bridges decreased the extent of molecular interdigitation,[5] there was a tendency for one of the bridges to collapse toward the central phenylene, ultimately hindering the desired rotation.

The tendency for a bridge to collapse toward the rotator inspired us to explore the use a photoactivatable bridging group that might serve as a simple molecular brake, which may help modify the rotational dynamics of the molecule (Figure 1B). Based on its similarity with the previously studied benzophenone bridges, and the previous work in the field using the azobenzene chromophore,[6] we selected a 4,4′-dimethylazobenze as a photoresponsive molecular bridge. We report here the synthesis, characterization, photochromic behavior, and rotational dynamics of the singly azobenzene bridged molecular gyroscope **2**. Although we encountered challenges associated with the desolvation and lack of reactivity of single crystals grown from dichloromethane and diethyl ether, we showed that nanocrystals obtained by precipitation of a THF solution of *trans*-**2** in water led to photoactive crystals, which were photochemically investigated in the form of nanocrystalline suspensions. The polymorphic nature of the nanocrystals was determined by PXRD, their habits analyzed by scanning electron microcopy (SEM), and the remarkable thermal stability of the photogenerated *cis*-azobenzene isomer established by UV−vis absorption methods. Using solid state $^2$H NMR of filtered nanocrystals, we were able to confirm that rotational exchange dynamics in the original *trans*-**2** structure

**Received:** November 13, 2013
**Published:** January 15, 2014

   dx.doi.org/10.1021/jo402516n | J. Org. Chem. 2014, 79, 1611−1619

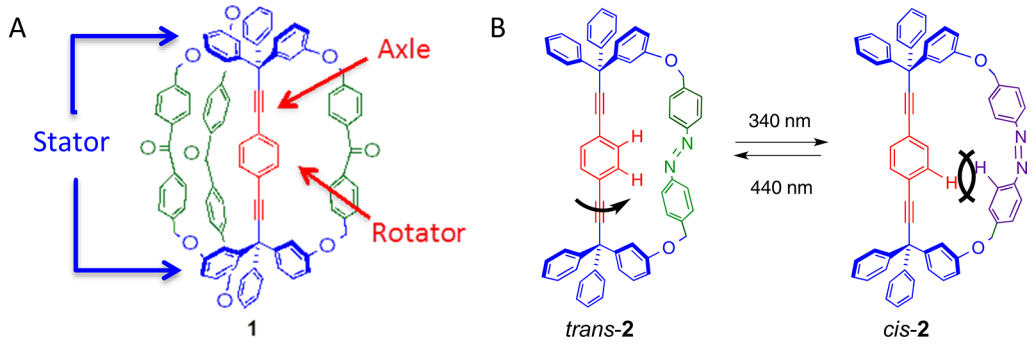


**Figure 1.** (A) A molecular gyroscope with three benzophenone bridges. (B) An idealized model of an azobenzene bridged molecular gyroscope where a change from *trans*- to *cis*-azobenzene configurations may change the rotational motion of the central phenylene.

**Scheme 1**

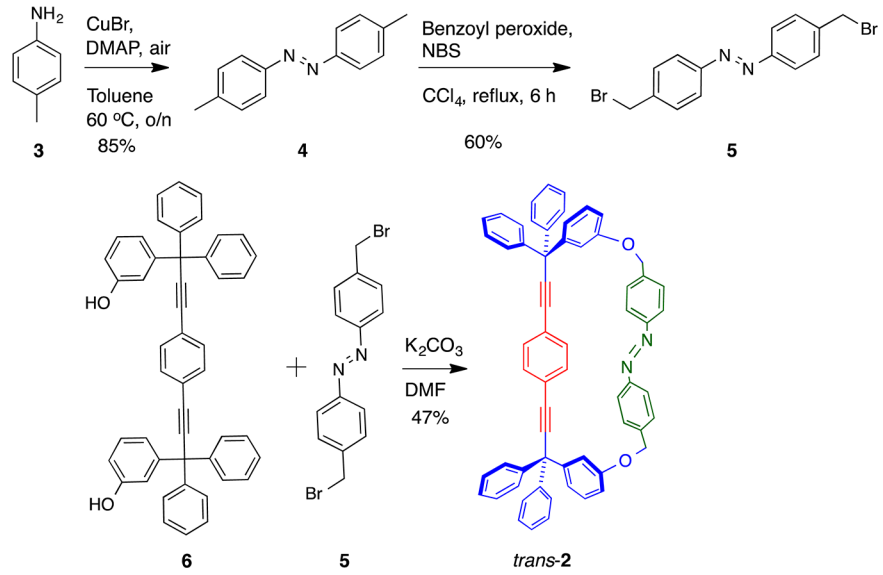


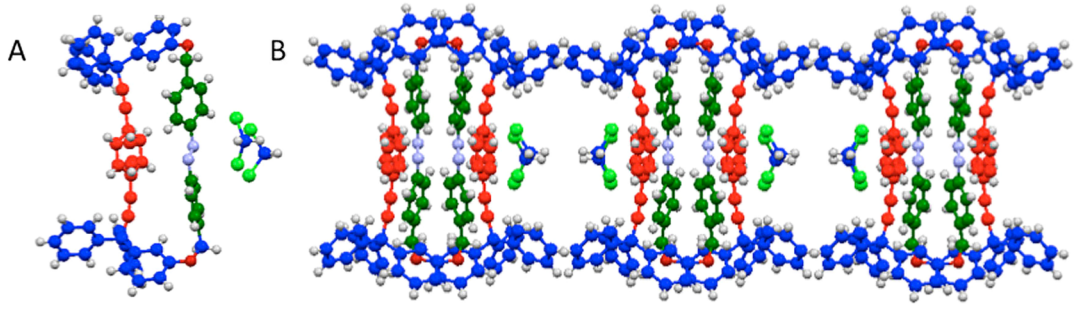


**Figure 2.** (A) X-ray-determined molecular structure of *trans*-**2** as a dichloromethane solvate. (B) Packing of *trans*-**2** in sheets made with pairs of molecules having adjacent azobenzene bridges on one side and creating a cavity for two molecules of dichloromethane on the other.

has a lower energy barrier than that of the metastable *cis*-**2** form.

## RESULTS AND DISCUSSION

**Synthesis and Characterization.** The synthesis of *trans*-**2** was achieved using the convergent synthesis shown in Scheme 1. Samples of 1,2-bis(4-(bromomethyl)phenyl)diazene **5** were obtained from *p*-toluidine **3** using CuBr(I) and dimethylaminopyridine (DMAP) in air to afford 4,4′-dimethylazobenzene **4**.[7] Compound **4** was then doubly brominated by refluxing *N*-bromosuccimide (NBS) and benzoyl peroxide in carbon tetrachloride for 6 h to afford **5** in 60% yield.[8]

The azobenzene bridged molecular gyroscope *trans*-**2** was prepared by slow addition of **5** and diphenol molecular rotor **6** into a flask with potassium carbonate in DMF to provide high dilution conditions (1.0 mM based upon **6**) to favor macrocyclization. The bridged molecular gyroscope *trans*-**2** was obtained in a 47% yield, or 69% yield per bond formed, which is in good agreement with previous macrocyclization reactions.[5] A deuterated isotopologue was also synthesized to study the rotational dynamics of *trans*-**2** and *cis*-**2** using quadrupolar spin−echo $^{2}$H NMR spectroscopy. The isotopologue *trans*-**2**-$d_4$ was synthesized in the same manner using 1,4-dibromobenzene-$d_4$ instead of 1,4-diiodobenzene in the


dx.doi.org/10.1021/jo402516n | J. Org. Chem. 2014, 79, 1611−1619

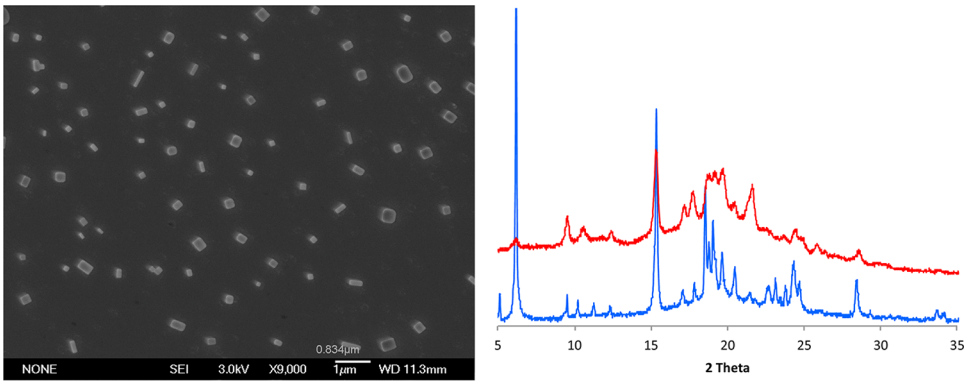


**Figure 3.** (Left) SEM image of nanocrystals of *trans*-**2** formed by the reprecipitation method. The particles are well faceted and have an average size of ca. 96 nm. (Right) PXRD spectrum of filtered nanocrystals of *trans*-**2** (red line) and the experimental PXRD spectrum of desolvated crystals *trans*-**2** crystallized from dichloromethane and diethyl ether (blue line).

Sonogashira coupling.[5] The resulting *trans*-**2** (and *trans*-**2**-$d_4$) were purified by column chromatography and characterized by $^{13}$C NMR, $^1$H NMR, attenuated total reflectance (ATR) FTIR, and high-resolution mass spectrometry. By $^1$H NMR, compound *trans*-**2** showed the expected AA′BB′ spin system associated with the 1,4-disubstituted azobenzene bridge at 7.84 and 7.38 ppm, a 1,3-disubstituted aryl splitting pattern from the trityl stator, and the only nonaromatic signal is a singlet located at 5.20 ppm from the benzylic methylene protons of the azobenzene bridge. A diagnostic singlet at 6.84 ppm was attributed to the four phenylene protons of the motionally averaged rotator. Upon irradiation with 340 nm UV light to generate the *cis*-**2** isomer, we noticed that the AA′BB′ spin system of the azobenzene bridge showed an upfield shift to the heavily populated aromatic region between 7.40 and 6.91 ppm. The methylene singlet also experienced an upfield shift to 4.91 ppm, which was a useful diagnostic to determine the ratio between the two isomers. The $^1$H NMR spectra for both the *trans*-**2**-$d_4$ and *cis*-**2**-$d_4$ are nearly identical to the natural abundance samples, except that the phenylene rotator singlets are no longer present.

**Crystallization Studies.** Diffraction quality single crystals of *trans*-**2** were obtained by slow evaporation of a 1:1 solution of dichloromethane and diethyl ether. The diffraction data was acquired at 100 K and solved in the monoclinic system, space group $P2_1/c$ with four molecules of *trans*-**2** and ca. 3.3 molecules of dichloromethane per unit cell (Figure 2A). The position of the phenylene rotator is disordered over two sites with occupancies of 73% and 27% that differ by an angle of 37°. The molecular structure is characterized by a conformation where the three C−Ar bonds on the two trityl groups adopt a staggered orientation and adopt angles that result in the same axial chirality. The two alkynes are bent such that the central phenylene rotator is bowed toward the azobenzene nitrogens. The two aryl rings that compose the azobenzene moiety are twisted 39° away from planarity. The molecular gyroscopes pack in layers in a manner that is similar to that observed for several previously reported bridged structures.[5,9] Each molecule has one of its two trityl groups engaged in a sixfold phenyl embrace.[10] The other trityl group is slightly offset from its neighboring trityl group, preventing a sixfold phenyl embrace, but forming two edge-to-face interactions. There is one molecule of dichloromethane disordered over two sites with occupancies of 46% and 37% located in the space between the pairs of molecular gyroscopes (Figure 2b). The 17% of solvent that is not accounted for is presumed to have evaporated before or while the structure was acquired. There is an intermolecular close contact between a proton in the phenylene rotator and two of the azobenzene carbons of 2.6 Å and 2.7 Å. There is an additional intermolecular close contact of 3.1 Å present between one of the methylene protons and a carbon of a neighboring trityl stator.

**Nanocrystalline Suspensions.** To study the photoisomerization of *trans*-**2** in the solid state, we decided to explore the formation of nanocrystalline suspensions in water. It has been shown that suspended nanocrystals constitute an ideal medium to analyze solid state photochemical reactions with conventional transmission spectroscopy methods. When their size is smaller than the wavelength of light, suspended crystals may be compared with large proteins or protein complexes, and many of the challenges associated with bulk solids, which are related to their high optical density, birefringence, and light scattering, are strongly diminished.[11]

Nanocrystalline suspensions of *trans*-**2** were obtained from THF and water by the reprecipitation method (also known as solvent-shift method), which consists of the addition of a concentrated solution of the desired compound in a good water-miscible solvent into vigorously stirring water.[12] The nanocrystalline suspensions of *trans*-**2** were analyzed by dynamic light scattering (DLS) and SEM. Nanocrystalline specimens were shown to have an average size of ca. 96 nm by DLS (Figure S20), which was in good agreement with the size of crystals observed in the SEM image shown in Figure 3. The image also revealed that nanocrystals are well faceted and have a rectangular habit. To determine the nature of nanocrystals of *trans*-**2** obtained from THF−water, we measured their powder X-ray diffraction (PXRD). Their diffractogram is shown in Figure 3 along with the one obtained with powdered crystals grown from $CH_2Cl_2$. Not surprisingly, the two diffractograms do not match and the one obtained from the filtered nanocrystals reveals significantly broader peaks, consistent with the very small size of the nanocrystalline specimens,[13] and a very broad baseline indicating that at least part of the filtrate is amorphous. It is important to note that both the nanocrystalline suspension and the bulk powder of *trans*-**2**-$d_4$ contain >97% of *trans* isomer, so the difference in the diffraction data is not attributed to different contributions of the *cis* isomer. While numerous crystallizations were attempted to obtain diffraction quality single crystals of *trans*-**2** by evaporation of tetrahydrofuran and water, only aggregates


dx.doi.org/10.1021/jo402516n | J. Org. Chem. 2014, 79, 1611−1619

could be obtained under those conditions. Crystallizations attempted by layering a solution of *trans*-**2** in THF on top of water yielded either conglomerates or very fine needles.

**Photoisomerization.** The photoisomerization of the azobenzene bridge molecular gyroscope *trans*-**2** was first studied by UV−vis spectroscopy in a dilute benzene solution and then as a nanocrystalline suspension in water. The UV−vis of *trans*-**2** shows the typical $\pi\rightarrow\pi^*$ and $n\rightarrow\pi^*$ transition of azobenzene at ca. 340 and 440 nm, respectively.[14] There is also a very strong absorbance located at 290 nm (not shown) attributed to the benzene chromophores in the two trityl groups. Irradiation of *trans*-**2** in solution at 340 nm for various time increments resulted in the diagnostic decrease in the absorbance of the 340 nm band, which was accompanied by a slight increase of the absorption band at 440 nm, as expected for the isomerization of *trans*-**2** to the *cis*-**2** (Figure 4 top

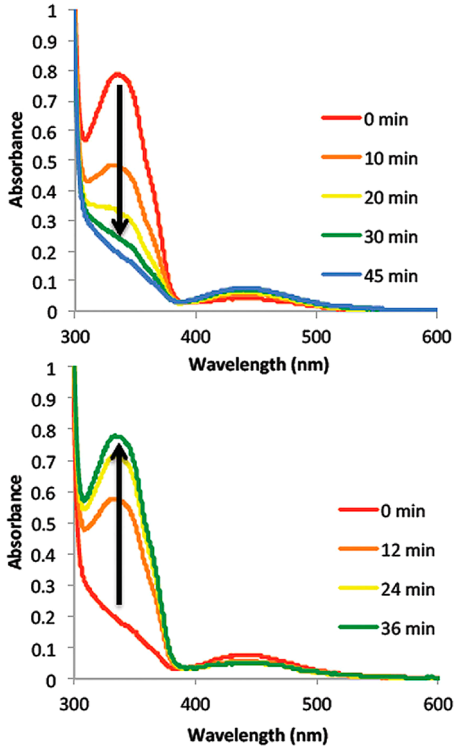


**Figure 4.** (Top) The photoisomerization of *trans*-**2** to *cis*-**2** in benzene upon irradiation at 340 nm until it reaches a photostationary state, and (Bottom) preferential photoisomerization of *cis*-**2** to *trans*-**2** by irradiation at 440 nm and return to the *trans*-**2** form.

frame). Analysis of a sample that had reached its photostationary state as judged by change in its UV−vis spectrum was evaluated by $^1$H NMR, which established a *trans*:*cis* ratio of 26:74. Irradiation of a sample that had reach the photostationary state at $\lambda$ = 440 nm, where *cis*-**2** can be preferentially excited, showed a rapid recovery of the absorption band at 340 nm such that the sample returned to its initial state after only ca. 36 min (Figure 4, bottom frame).

In contrast to the changes observed in solution, exposure of the dry dichloromethane-containing crystals of *trans*-**2** to UV light for up to 24 h revealed no changes in the UV−vis spectrum. Since there are many examples of photoactive azobenzene chromophores in the solid state,[6,14] it seems reasonable that the photostable nature of these crystals may be due to self-quenching arising from tight face-to-face interaction between pairs of azobenzene moieties in the crystal, or it could also be due to the crowded environment surrounding azobenzene, which has several close contacts in its crystal environment. To our surprise, when analogous experiments were carried out with nanocrystalline suspensions, we discovered that the *trans*−*cis* photoisomerization takes place as it does in solution (Figure 5), but under otherwise similar

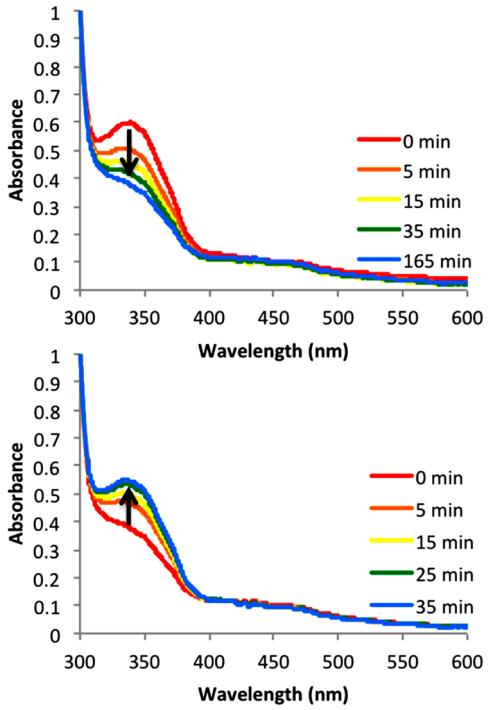


**Figure 5.** (Top) Photoisomerization of nanocrystalline *trans*-**2** to *cis*-**2** upon irradiation at 340 nm until it reaches a photostationary state, and (Bottom) preferential photoisomerization of *cis*-**2** to *trans*-**2** by irradiation at 440 nm.

conditions, it appeared to be significantly slower. A photostationary state was reached after exposing the sample to UV light for approximately 165 min, and the reduction in the maximum absorbance at 340 nm was only 46% as compared to the change observed in solution. This change corresponds to a *trans*:*cis* photostationary state of 66:34, which was confirmed by $^1$H NMR analysis (Figure S21). Conversion of *cis*-**2** to *trans*-**2** by irradiation at 440 nm was shown as a relatively fast increase in the absorption band at 340 nm, such that continued irradiation returns the sample to the *trans*-**2** isomer within 34−40 min (Figure 5 bottom frame).

**Thermal Reversibility.** The thermal equilibration of *cis*-**2** back to *trans*-**2** was analyzed by measuring the recovery of the intense absorption of *trans*-**2** at 334 nm. An aqueous nanocrystalline suspension of *trans*-**2** was irradiated at 365 nm until it reached its photostationary state after 120 min. The suspension was monitored by UV−vis absorption at 334 nm after intervals of 10 to 20 h for a total of 340 h at room temperature, when ca. 60% of the original absorption value had been recovered. At that time, the sample was exposed to broad visible light and full recovery was observed after a few minutes, indicating that it had the potential of going back to the original state but was undergoing a very slow thermal isomerization process. While the data is insufficient for a rigorous kinetic analysis, it was clear that a fit of the thermal isomerization data


dx.doi.org/10.1021/jo402516n | J. Org. Chem. 2014, 79, 1611−1619

would require a model with at least two components recovering with very different rates, with the fast component being relatively minor (Figure S22). Assuming that full thermal recovery would occur after very long times, the data could be fit reasonably well by a short component of 19.9 h and a long component of 330 h (13.75 days) with weighted contributions of 0.7% and 99.3%, respectively (Figure S23). This result indicated that the long lifetime of the metastable *cis*-**2** form should make it possible to study the rotational dynamics of the central phenylene-$d_4$ for both the stable (100% *trans*-**2**) and metastable (34% *cis*-**2**) forms using the slow quadrupolar echo $^2$H NMR technique, which can take tens of hours. For simplicity, for the remainder of this paper, we will refer to metastable crystals containing *ca.* 34% *cis*-**2** just as "*cis*-**2**".

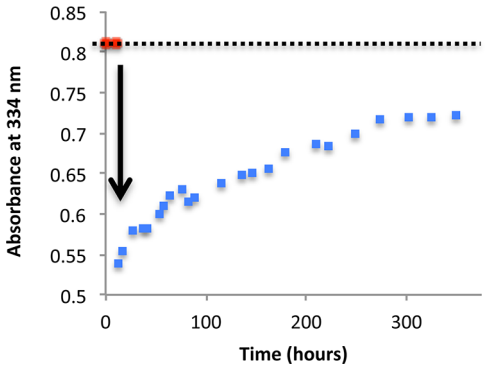


**Figure 6.** Thermal isomerization of nanocrystalline *cis*-**2** into *trans*-**2** determined by measuring the recovery of the UV−vis absorption the as a function of time. The two red dots indicate the absorbance before UV irradiation at $\lambda$ = 365 nm.

The photochemical stability of the azobenzene bridge was evaluated by multiple isomerization cycles both in benzene (not shown) and as a nanocrystalline suspension in water (Figure 7).

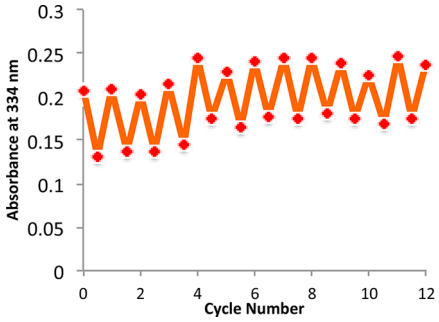


**Figure 7.** Changes in absorbance of suspended nanocrystals of *trans*-**2** alternatively irradiated with 365 nm and white light. A similar behavior with a greater change on optical densities was observed in solution.

Azobenzene is a robust chromophore, capable of undergoing hundreds of isomerization cycles without significant photodegradation.[6] When exposed to 365 nm light for 15 min and allowed to re-equilibrate under ambient light for 12 h, molecular gyroscope **2** showed good cyclability over 12 cycles both in solution and as a nanocrystalline suspension (Figure 7).

**Variable Temperature $^2$H Spin−Echo NMR Analysis.** Deuterium NMR is a powerful technique for determining rotational dynamics in the solid state.[15] It relies on the use of samples labeled with deuterium atoms in positions where motion will be probed, the central phenylene rotator in our case. The $^2$H NMR spectrum is dominated by the interaction between the nuclear spin and the electric quadrupole moment at the nucleus. It has an orientation dependence that makes it sensitive to dynamics in the range of ca. $10^3$ to $10^8$ $s^{-1}$. Each deuteron provides a doublet with a splitting frequency $\Delta\nu$ that depends on the orientation angle $\beta$ that the C−$^2$H bonds make with respect to the external field:

$$\Delta\nu = 3/4(e^2q_{zz}Q/h)(3\cos^2\beta - 1)$$
$$= 3/4\mathrm{QCC}(3\cos^2\beta - 1)$$

The magnitude of $\Delta\nu$ for deuterons with an axially symmetric electric field gradient tensor depends on the electric quadrupole moment of the deuteron, $Q$, and on the magnitude of the principal component of electric field gradient tensor, $q_{zz}$, which lies along the C−$^2$H bond. Combined with the electric charge and Plank constant, $e$ and $h$, the first term in the equation represents the quadupolar coupling constant QCC, for which we have used a value 180 kHz for aromatic deuterons. Static powder samples have all the $\beta$ angles represented and consist of a combination of doublets with populations and intensities that reflect a statistical distribution with respect to the external field, known as a Pake pattern (Figure 8a). The corresponding broad symmetric spectrum characterized by two sharp maxima and two feet separated by ca. 125 kHz and 250 kHz, respectively, as shown in Figure 8a. By contrast, powder samples with phenylene groups undergoing a fast site exchange described as 180° rotations are subject to dynamic averaging and result in a narrower symmetric spectrum with the two maxima separated by distance of only ca. 32 kHz and two sets of shoulders with separations of ca. 115 and 150 kHz (Figure 8d). Spectral changes caused by 180° rotation in the intermediate exchange regime denote an evolution between the two limits as illustrated with the examples in Figure 8b and c. Importantly, several excellent programs are available to simulate these spectra with models that include sites with variable flip angles, populations, and energy barriers.[16] In addition, there are also other groups modeling the theoretical dynamics of molecular gyroscopes using computational chemistry.[17]

Measurements of nanocrystalline samples of *trans*-**2** and *cis*-**2** were carried out at 46.07 MHz with a 90° pulse width of 2.5 $\mu$s, echo and refocusing delays of 50 and 42 $\mu$s, respectively, using a 15 s delay for relaxation between pulses. Samples of nanocrystals of *trans*-**2** were prepared using the reprecipitation method,[12] centrifuged, decanted, and the resulting pellet was dried in a desiccator at 298 K for 24 h. Samples of *cis*-**2** were prepared in the same manner, except that the nanocrystalline suspension was exposed to light at $\lambda$ = 365 nm for 4 h prior to centrifugation.

Samples of *trans*-**2** were measured between 170 and 296 K, but only those acquired below 220 K are shown in the left column in Figure 9. Spectra acquired above 220 K were characteristic of rotational motion in the fast exchange regime with some additional narrowing mechanism (please see below). Similarly, nanocrystals of *cis*-**2** were analyzed in the range of 200−260 K as illustrated on the right column of Figure 9. As in the case of *trans*-**2**, spectra acquired at higher temperatures displayed further narrowing that deviates from a twofold flipping process and were analyzed further. One can see that the spectra measured at any given temperature are different for the two samples, indicating that the motion of pure *trans*-**2** is indeed affected by the partial isomerization into the *cis*-isomer. This is evident in the spectra measured at 220 K where one can


dx.doi.org/10.1021/jo402516n | J. Org. Chem. 2014, 79, 1611−1619

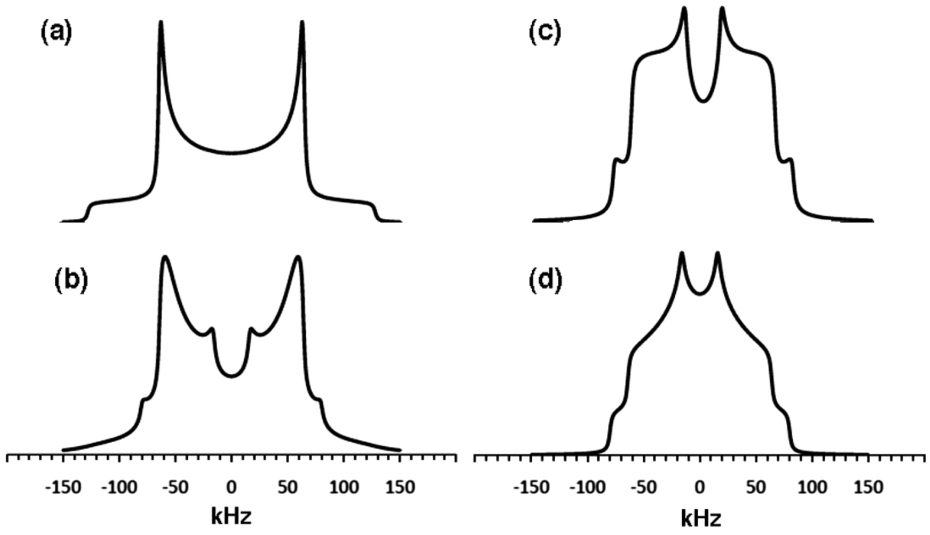


**Figure 8.** Examples of simulated $^2$H NMR spectra corresponding to phenylene deuterons undergoing two-site 180° flips with exchange frequencies of (a) $k_{ex} \leq 10^3$ s$^{-1}$, (b) $k_{ex} = 10^5$ s$^{-1}$, (c) $k_{ex} = 10^6$ s$^{-1}$, and (d) $k_{ex} \geq 10^8$ s$^{-1}$ with a quadrupolar coupling constant of 180 kHz and an asymmetry parameter $\eta = 0$.

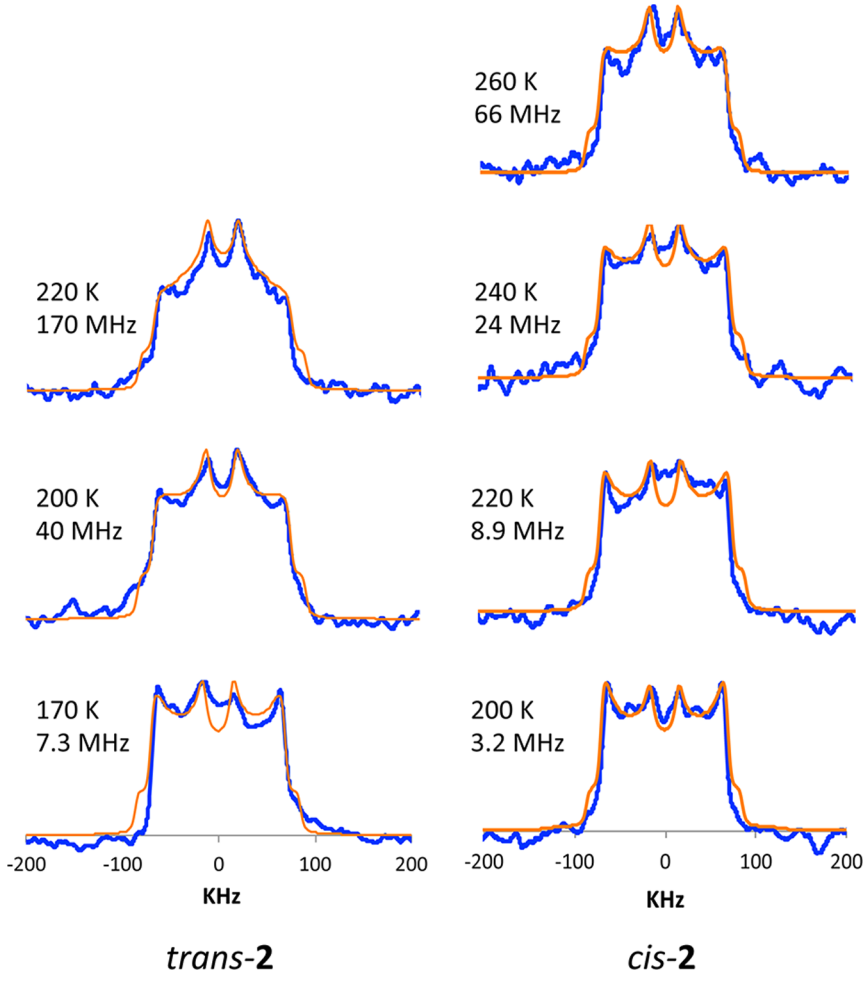


**Figure 9.** Spin−echo $^2$H NMR spectra for nanocrystals of the *trans*-**2** (left) and *cis*-**2** (right) isomers. The heavy blue line represents the experimental data and the thin orange line indicates the spectra simulation, obtained as described in the text. The mean rotational rate used for each fitting is listed next to the corresponding spectrum. A line broadening of 5 kHz was used during processing.

see that rotation in crystals of *trans*-**2** is already in the fast exchange regime ($k_{ex} \geq 10^8$ s$^{-1}$) while rotation in crystals containing *cis*-**2** remains at intermediate values, clearly showing that solid state isomerization leads to more hindered rotation.


dx.doi.org/10.1021/jo402516n | J. Org. Chem. 2014, 79, 1611−1619

The spectra shown in Figure 9 are generally consistent with the expected twofold flipping process, but there are features indicating the coexistence of sites where rotation occurs with faster and slower exchange rates. The co-occurrence of fast and slow sites in the sample can be deduced from spectra that contain peaks characteristic of the two dynamic ranges. For example, the spectrum of *trans*-**2** measured at 170 K has two sets of maxima separated by ca. 125 and 32 kHz, which may be approximated as a sum of spectra such as those shown in Figure 8a and d. Spectra measured at higher temperatures display an increasing contribution from the faster components as seen by the greater intensity of the two inner peaks. Recognizing the solid has an amorphous component as indicated by PXRD, the heterogeneous nature of the spectra is unsurprising, and we explored a model that involves two discrete sites with different dynamics and a model that describes a system with a distribution of sites and activation energies leading to a distribution of exchange rates. The $^2$H NMR simulations were performed using the program Express 1.0.[16b] with a quadrupolar coupling constant of 180 kHz and an asymmetry parameter of $\eta = 0$. Attempts to use a simple two-site model generally gave unsatisfactory results. The most reasonable simulations of the *trans*-**2** spectra shown in Figure 9 required a model based on log-Gaussian distribution of jump rates with a width of $\sigma = 1.5$. The simulations gave a reasonable match to the experimental spectra with exchange frequencies of 7.3, 40, and 170 MHz for data acquired at 170, 200, and 220 K, respectively. Arrhenius analysis revealed an average activation energy $E_a = 4.6 \pm 0.6$ kcal/mol and a pre-exponential factor of exp(29.42 ± 1.71) $s^{-1}$ (Figure 10, top).

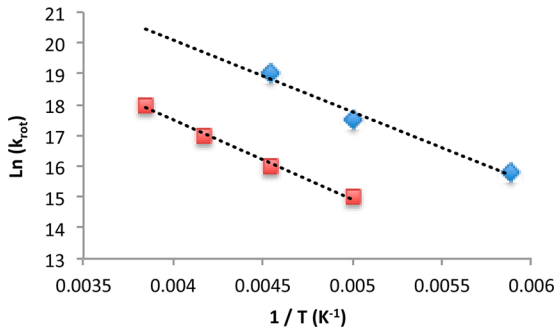


**Figure 10.** Arrhenius plots derived from the variable temperature spin−echo $^2$H NMR data and simulations of *trans*-**2** (blue diamonds) and *cis*-**2** (red squares). The activation energy and pre-exponential factors for *trans*-**2** are 4.6 ± 0.6 kcal/mol and exp(29.42 ± 1.71) $s^{-1}$, and those for *cis*-**2** are 5.1 ± 0.6 kcal/mol, and exp(27.86 ± 1.32) $s^{-1}$, respectively.

The spectra of *trans*-**2** acquired above 230 K had an appearance that indicate an exchange process beyond the fast exchange regime for a 180° rotation with noticeable narrowing as the temperature increased up to 296 K (Figure 11A). We considered that the observed narrowing may be explained by increasingly larger oscillations of the phenylene rotator by an angle Δ°, in addition to the discrete 180° flips. The effects of increasing angular displacements (Δ°) on the appearance of the spectrum were explored with simulations of twofold flipping motions in the fast exchange regime (>$10^8$ Hz) with added oscillations between Δ = 0° and Δ = 60°, as shown in Figure 11B.[18] One can see that the experimental spectrum acquired at 230 K resembles simulations with oscillations in the range of 0−10°. However, the data obtained at 296 K is much narrower on the top than on the bottom, and does not resemble any of the simulated librations. We interpret the spectral changes in Figure 11A as a function of increasing temperature as resulting from a heterogeneous distribution of large librational amplitudes. This interpretation is in agreement with the sample heterogeneity displayed in the PXRD and by the need for a log-Gaussian model to simulate the spectra obtained in the intermediate regime.

The spectra of nanocrystals of *cis*-**2** were acquired at 200−296 K (Figure 9). The spectra were also simulated using a weighted average of a log-Gaussian distribution of jump rates, but a distribution width of $\sigma = 2.0$ was necessary to obtain a good fit. Since the irradiated *cis*-**2** nanocrystals are a 31:69% solid solution of *cis*-**2** and *trans*-**2** isomers, a more heterogeneous mixture of activation energies would be expected and this assumption is reflected in the line-shape analysis simulation, which required a $\sigma = 2$ value. The exchange frequencies were simulated to be 3.2, 8.9, 24, and 66 MHz for data acquired at 200, 220, 240, and 260 K, respectively. It is important to note that the thermal *cis* to *trans* isomerization during the acquisition of the spectra was considered to be small because the lifetime of the thermal isomerization was estimated to be almost fourteen days (330 h) at 296 K, and the acquisition of each spectrum was approximately 12 h at temperatures that are 30−96 K lower, where the lifetime should be much longer. The $^2$H NMR calculated mean activation energy for rotation of *cis*-**2** is 5.1 ± 0.6 kcal/mol, which is 0.5 kcal/mol higher than the barrier for the *trans* isomer and the pre-exponential factor is exp(27.86 ± 1.32) $s^{-1}$. Noticing that there is an overlap between the margin of error and calculated difference between the two isomers, further statistical anaylysis was performed and the data was determined to have a *z*-score of 0.98, indicating that there is a confidence level of 84% that the data is significant. In addition to the relatively small differences in activation barriers, an almost 10-fold difference in exchange frequencies for *trans*-**2** and *cis*-**2** in the range of 200−220 K can be traced to differences in the two mean pre-exponential factors, which differ by a factor of 4.6. One of the factors previously shown to lower the pre-exponential factor of a molecular rotor is the amorphicity of the sample,[19] which in this case is consistent with the high heterogeneity displayed by the *cis*-**2** isomer, which required a kinetic model with a wider barrier distribution width. Unfortunately, a single crystal X-ray structure of the phase corresponding to the nanocrystalline solid could not be obtained, so the structural details that may be related to different rotational rates cannot be determined.

## ■ CONCLUSION

While good quality dichloromethane-containing single crystals of *trans*-**2** could be used to confirm its molecular and packing structure by single crystal X-ray diffraction determination, they were shown to be photostable. By contrast, nanocrystalline specimens obtained by solvent shifting from saturated THF to water resulted in a photochemically active solvent-free pseudopolymorph. Nanocrystalline samples of *trans*-**2** displayed promising photochemical reversibility, and the thermal stability of the photogenerated *cis*-**2** isomer was shown to be considerable. The rotational dynamics measurements by spin−echo $^2$H NMR with filtered nanocrystals showed that spectra obtained as a function of temperature could only be simulated with a model that considers a Gaussian distribution of activation energies centered at 4.6 ± 0.6 kcal/mol with a


dx.doi.org/10.1021/jo402516n | J. Org. Chem. 2014, 79, 1611−1619

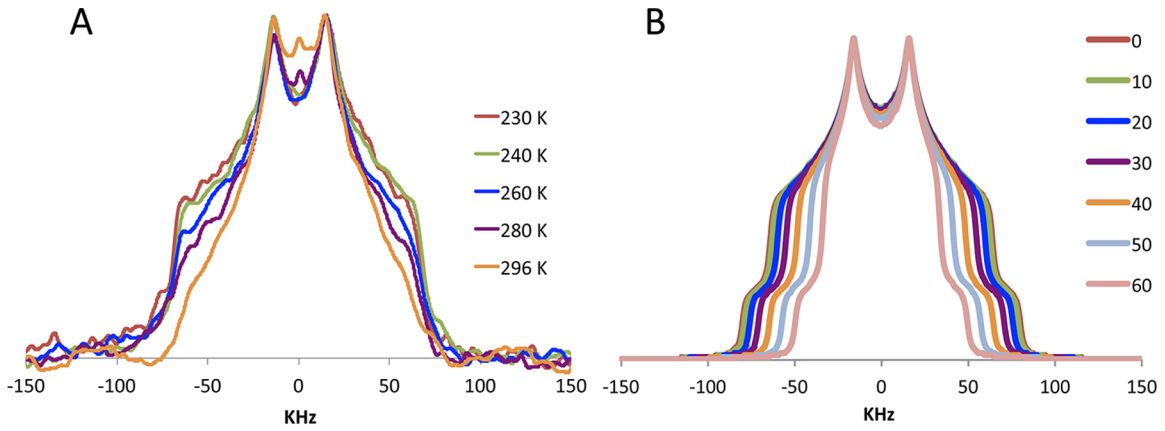


**Figure 11.** (A) Quadupolar spin echo $^2$H NMR of *trans*-**2** measured between 230 and 296 K showing an increasing narrowing of the spectrum. (B) Simulations of a model based on a twofold flipping in the fast exchange regime with increasing varying degrees of librational motion with angular displacement ranging from 0° to 60°.

width $\sigma$ = 1.5, while *cis*-**2** has a higher activation energy centered at 5.1 ± 0.6 kcal/mol with a broader distribution indicated by width of $\sigma$ = 2.0. While the exact underlying mechanism responsible for the different rotational states cannot be ascertained without detailed structural knowledge, this study shows that carefully designed functionalization of molecular gyroscopes may lead to molecules with rotational dynamics that are amenable to control by external stimuli, a feature of high promise in the field of crystalline molecular machines.

## EXPERIMENTAL SECTION

All commercially available compounds were used without further purification. Samples of 4,4′-dimethylazobenzene **4** and 1,2-bis(4-(bromomethyl)phenyl)diazene **5** were prepared as described in the literature.[7,8]

**Azobenzene Bridged Molecular Gyroscope, 2.** A 100 mL round-bottom flask equipped with a magnetic stir bar was charged with potassium carbonate (82 mg, 0.6 mmol) and dry DMF (50 mL) and put under Ar: dissolved **5** (55 mg, 0.15 mmol) and **6**-$d_4$ (96 mg, 0.15 mmol) in dry DMF (4 mL) in separate round bottoms under Ar; added **5**, and **6**-$d_4$ to the reaction at a rate of 0.5 mL per hour for 8 h. The reaction was stirred at 40 °C for 24 h. The organic phase was partitioned with DCM, and washed with saturated aqueous LiCl (3 × 50 mL), water (50 mL) and brine (50 mL). The combined organic fractions were dried over $MgSO_4$ and concentrated on a rotary evaporator. The residue was then purified by flash chromatography on silica gel (1:1 hexanes:DCM) to afford 60 mg (47%) of yellow powder. Mp = 295−296 °C. HRMS ESI-TOF(+) calcd. for $[C_{62}H_{45}N_2O_2]^+$: 849.3481; Found: 849.3492 (M+H).

*trans-**2**: FTIR (solid, HATR, cm$^{-1}$).* 3060, 2923, 2852, 2247, 1714, 1595, 1488, 1259, 1230, 1033, 906, 729, 696. $^1$H NMR *trans* (300 MHz, $CDCl_3$): $\delta$ 7.84 (d, $J$ = 8.7 Hz, 4H), 7.38 (d, $J$ = 8.2 Hz, 4H), 7.35−7.27 (m, 20H), 7.11 (apparent triplet, $J$ = 8.2, 7.8 Hz, 2H), 6.99 (ddd, $J$ = 8.2, 2.5, 0.9 Hz, 2H), 6.84 (s, 4H), 6.82 (dd, $J$ = 2.5, 1.8 Hz, 2H), 6.25 (ddd, $J$ = 7.8, 1.8, 0.9 Hz 2H) 5.20 (s, 4H). $^{13}$C NMR (100 MHz, $CDCl_3$): 158.2, 151.8, 145.8, 145.0, 140.8, 131.2, 129.1, 128.7, 128.0, 127.2, 126.7, 123.1, 122.7, 121.7, 117.5, 115.4, 96.3, 85.0, 69.9, 56.2.

*cis-**2**: FTIR (solid, HATR, cm$^{-1}$).* 3060, 2923, 2853, 1720, 1596, 1488, 1447, 1238, 1033, 907, 791, 729, 696. $^1$H NMR (300 MHz, $CDCl_3$): $\delta$ 7.64 (dd, $J$ = 2.5, 1.9 Hz, 2H), 7.43 (s, 4H), 7.3−7.20 (m, 24H), 7.17 (apparent triplet, $J$ = 8.0, 8.0 Hz, 2H), 6.90 (ddd $J$ = 8.0, 1.9, 0.7 Hz, 2H) 6.89 (d, $J$ = 8.5 Hz, 4H), 6.41 (ddd, $J$ = 8.0, 2.5, 0.7 Hz, 2H), 4.91 (s, 4H). $^{13}$C NMR (125 MHz, $CDCl_3$): 158.8, 153.0, 146.9, 145.0, 144.9, 135.9, 129.1, 128.6, 128.1, 127.0, 126.98, 126.92, 126.9, 121.9, 120.8, 115.6, 113.1, 97.4, 84.9, 69.9, 56.3.

*Azobenzene Bridged Molecular Gyroscope-$d_4$, trans-**2**-$d_4$.* A 100 mL equipped with a magnetic stir bar was charged with potassium carbonate (82 mg, 0.6 mmol) and dry DMF (50 mL) and put under Ar: dissolved **5** (55 mg, 0.15 mmol and **6**-$d_4$ (96 mg, 0.15 mmol) in dry DMF (4 mL) in separate round bottoms under Ar; added **5**, and **6**-$d_4$ to the reaction at a rate of 0.5 mL per hour for 8 h. The reaction was stirred at 40 °C for 24 h. The organic phase was diluted with DCM, and washed with saturated aqueous LiCl (3 × 50 mL), water (50 mL), and brine (50 mL). The combined organic fractions were dried over $MgSO_4$ and concentrated on a rotary evaporator. The residue was then purified by flash chromatography on silica gel (1:1 hexanes:DCM) to afford 54 mg (42%) of yellow powder. Mp = 295−296 °C. HRMS ESI-TOF(+) calcd for $[C_{62}H_{41}D_4N_2O_2]^+$: 853.3732; Found: 853.3729 (M+H).

*trans-**2**-$d_4$: FTIR (solid, HATR, cm$^{-1}$).* 3059, 2925, 1728, 1595, 1488, 1447, 1260, 1230, 1033, 906, 729, 696. $^1$H NMR *trans* (400 MHz, $CDCl_3$): $\delta$ 7.84 (d, $J$ = 8.2 Hz, 4H), 7.38 (d, $J$ = 8.2 Hz, 4H), 7.35−7.27 (m, 20H), 7.11 (apparent triplet, $J$ = 8.2, 7.8 Hz, 2H), 6.99 (ddd, $J$ = 8.2, 2.5, 0.9 Hz, 2H), 6.84 (s, 4H), 6.82 (dd, $J$ = 2.5, 1.8 Hz, 2H), 6.27 (ddd, $J$ = 7.8, 1.8, 0.9 Hz 2H) 5.20 (s, 4H). $^{13}$C NMR *trans* (125 MHz, $CDCl_3$): 158.1, 151.7, 146.8, 145.0, 140.8, 131.7 (t, $J_{CD}$ = 25 Hz), 129.1, 128.7, 128.0, 127.2, 126.8, 123.1, 122.7, 121.7, 117.0, 115.4, 96.3, 84.9, 69.9, 56.1.

*cis-**2**-$d_4$: FTIR (solid, HATR, cm$^{-1}$).* 3055, 2925, 1596, 1488, 1447,1378, 1248, 1034, 908, 795, 757, 729, 696. $^1$H NMR *cis* (500 MHz, $CDCl_3$): $\delta$ 7.64 (dd, $J$ = 2.5, 1.9 Hz, 2H), 7.36 (d, $J$ = 8.5 4H), 7.3−7.20 (m, 20H), 7.17 (apparent triplet, $J$ = 8.0, 8.0 Hz, 2H), 6.90 (ddd $J$ = 8.0, 1.9, 0.7 Hz, 2H), 6.89 (d, $J$ = 8.5 Hz, 4H), 6.41 (ddd, $J$ = 8.0, 2.5, 0.7 Hz, 2H), 4.91 (s, 4H). $^{13}$C NMR *cis* (125 MHz, $CDCl_3$): 158.8, 153.0, 146.9, 144.9, 135.9, 131.1 (t, $J$ = 25, 1C) 129.1, 128.7, 128.6, 128.0, 127.0, 126.98, 123.0, 121.9, 120.8, 115.6, 113.1, 97.4, 84.9, 69.9, 56.3.

*1,4-Bis(3-(3-hydroxyphenyl)-3,3-diphenylpropynyl)benzene-$d_4$,* **6**-$d_4$. An oven-dried 250 mL round-bottom flask equipped with a magnetic stir bar was charged with **7** (2.21 g, 3.27 mmol) and dry DCM (30 mL) under an argon atmosphere. The flask was cooled to 0 °C in an ice bath, and 1 M $BBr_3$ in DCM (9.8 mL, 9.8 mmol) was added. The reaction was stirred for 3 h at 0 °C, quenched by addition of ice, and diluted with hexanes. The precipitate is filtered and washed with 0 °C DCM. Recovered 1.61 g (76%) of yellow powder. Compound was used in next step without further purification. FTIR (solid, HATR, cm$^{-1}$): 3531, 3356 (broad), 3058, 1591, 1488, 1446, 1262, 1183, 1031, 832, 781, 754, 697. $^1$H NMR (500 MHz, DMSO-$d_6$): $\delta$ 7.25−7.20 (m, 20H), 7.12 (apparent triplet, $J$ = 8.2, 7.8 Hz, 2H), 6.89 (dd, $J$ = 2.5, 1.8 Hz 2H), 6.78 (ddd, $J$ = 7.8, 1.8, 0.9 Hz 2H), 6.60 (ddd, $J$ = 8.2, 2.5, 0.9 Hz, 2H) 4.66 (s, 6H). $^{13}$C NMR (125 MHz, DMSO-$d_6$): $\delta$ 157.6 146.3, 145.0, 131.7 (t, $J_{CD}$ = 25 Hz) 129.6, 129.0, 128.7, 127.5, 122.8, 119.9, 116.3, 114.5, 97.7, 84.8, 56.2, 56.0. HRMS ESI-TOF(-) Calcd for $[C_{49}H_{30}D_4O_4]^-$ 691.2786; Found: 691.2783 (M +HCOO).


dx.doi.org/10.1021/jo402516n | J. Org. Chem. 2014, 79, 1611−1619

*1,4-Bis(3-(3-methoxyphenyl)-3,3-diphenylprop-1-yn-1-yl)-benzene-$d_4$, 7-$d_4$.* A 250-mL round-bottom flask equipped with a magnetic stir bar was charged with 3-(3-methoxyphenyl)-3,3-diphenylpropyne (1.1 g, 3.69 mmol), 1,4-dibromobenzene-$d_4$ (451 mg, 1.85 mmol), diisopropylamine (5 mL), dry THF (10 mL), CuI (35 mg, 0.18 mmol) and $Pd(PPh_3)_2Cl_2$ (130 mg, 0.18 mmol) added, and the reaction was heated to reflux for 48 h. The reaction was quenched with aqueous saturated ammonium chloride and partitioned with diethyl ether. The organic phase was washed with water (2 × 40 mL) and brine (40 mL). The combined organic fractions were dried over $MgSO_4$, filtered, and concentrated on a rotary evaporator. The residue was purified by flash chromatography on silica gel (2:1 hexanes:DCM) to afford 909 mg (73%) of a yellow solid: mp = 204–205 °C. FTIR (solid, HATR, $cm^{-1}$): 3056, 2930, 2831, 1601,1602, 1580, 1489, 1446, 1430, 1315, 1290, 1243, 1132, 1051, 881, 780, 756. $^1H$ NMR (400 MHz, $CDCl_3$): $\delta$ 7.36–7.22 (m, 22H), 6.95 (apparent triplet, $J$ = 8.2, 7.8 Hz, 2H), 6.90 (dd $J$ = 2.6, 1.5 Hz 2H), 6.86 (ddd, $J$ = 7.8, 1.8, 0.9, 2H), 6.82 (ddd, $J$ = 8.2, 2.5, 0.9, 2H), 3.75 (s, 6H). $^{13}C$ NMR (125 MHz, $CDCl_3$): $\delta$ 159.3, 146.8, 145.1, 131.1 (t, $J_{CD}$ = 25 Hz) 129.1, 128.9, 128.0, 126.9, 121.8, 115.5, 112.0, 97.3, 84.8, 56.2, 55.1. HRMS ESI-TOF(+) calcd for $[C_{50}H_{35}D_4O_2]^+$ 675.3201; Found: 675.3212 (M+H).

## ■ ASSOCIATED CONTENT

### Supporting Information

Spectroscopic data ($^1H$, $^{13}C$ NMR, FTIR) for compounds *trans*-**2**, *trans*-**2**-$d_4$, **7**, and **8**. Crystallographic information file (cif) for compound *trans*-**2**. Differential scanning calorimetry and thermogravimetric analysis for nanocrystals of *trans*-**2**, dynamic light scattering of nanocrystalline suspensions of *trans*-**2**, and decay kinetics for thermal isomerization of *cis*-**2**. This material is available free of charge via the Internet at http://pubs.acs.org.

## ■ AUTHOR INFORMATION


### Corresponding Author

*E-mail: mgg@chem.ucla.edu.


### Notes

The authors declare no competing financial interest.

## ■ ACKNOWLEDGMENTS

This work was supported by NSF IGERT: Materials Creation Training Program (MCTP) – DEG-0654431 and by grant DMR1101934. This material is based upon work supported by the National Science Foundation under equipment grant no. CHE-1048804.

## ■ REFERENCES


(1) (a) Koumura, N.; Zijlstra, R.; Delden, R.; Harada, N.; Feringa, B. *Nature* **1999**, *401*, 152. (b) Balzani, V.; Credi, A.; Raymo, F.; Stoddart, F. *Angew. Chem., Int. Ed.* **2000**, *39*, 3348. (c) Kelly, T. R.; De Silva, H.; Silva, R. A. *Nature* **1999**, *401*, 150. (d) Karim, A. R.; Linden, A.; Baldridge, K. K.; Siegel, J. S. *Chemical Science* **2010**, *1*, 102. (e) Muraoka1, T.; Kinbara1, K.; Aida, T. *Nature* **2006**, *440*, 512. (f) Coskun, A.; Banaszak, M.; Astumian, D. R.; Stoddart, J. F.; Grzybowski, B. A. *Chem. Soc. Rev.* **2012**, *41*, 19. (g) Browne, W. R.; Feringa, B. L. *Nat. Nanotechnol.* **2006**, *1*, 25. (h) Michl, J.; Sykes, E. C. H. *ACS Nano* **2009**, *3*, 1042. (i) Horie, M.; Suzaki, Y.; Hashizume, D.; Abe, T.; Wu, T. D.; Sassa, T.; Hosokai, T.; Osakada, K. *J. Am. Chem. Soc.* **2012**, *134*, 17932. (j) Lemouchi, C.; Iliopoulos, K.; Zorina, L.; Simonov, S.; Wzietek, P.; Cauchy, T.; Rodríguez-Fortea, A.; Canadell, E.; Kaleta, J.; Michl, J.; Gindre, D.; Chrysos, M.; Batail, P. *J. Am. Chem. Soc.* **2013**, *135*, 9366.

(2) (a) Khuong, T.-A. V.; Nuñez, J. E.; Godinez, C. E.; Garcia-Garibay, M. A. *Acc. Chem. Res.* **2006**, *39*, 413. (b) Karlen, S. D.; Garcia-Garibay, M. A. *Top. Curr. Chem.* **2006**, *262*, 179. Vogelsberg, C. S.; Garcia-Garibay, M. A. *Chem. Soc. Rev.* **2012**, *41*, 1892.

(3) Saebo, S.; Almolof, J.; Boggs, J. E.; Stark, J. G. *J. Mol. Struct. (Theochem)* **1989**, *200*, 361.

(4) (a) Han, J.; Deng, C.; Fang, R.; Zhao, D. Y.; Wang, L. Y.; Gladysz, J. A. *Organometallics* **2010**, *29*, 3231. (b) Hess, G. D.; Harnpel, F.; Gladysz, J. A. *Organometallics* **2007**, *26*, 5129. (c) Setaka, W.; Yamaguchi, K. *J. Am. Chem. Soc.* **2013**, *135*, 14560. (d) Setaka, W.; Yamaguchi, K. *J. Am. Chem. Soc.* **2012**, *134*, 12458. (e) Zeits, P. D.; Rachiero, G. P.; Harnpel, F.; Reibenspies, J. H.; Gladysz, J. A. *Organometallics* **2012**, *31*, 2854.

(5) Commins, P.; Nuñez, J. E.; Garcia-Garibay, M. A. *J. Org. Chem.* **2011**, *76*, 8355.

(6) (a) Kobatake, S.; Takami, S.; Muto, H.; Ishikawa, T.; Irie, M. *Nature* **2007**, *446*, 778. (b) Koshima, H.; Ojima, N.; Uchimoto, H. *J. Am. Chem. Soc.* **2009**, *131*, 6890. (c) Natanshohn, A.; Rochan, P. *Chem. Rev.* **2002**, *102*, 4139.

(7) Zhang, C.; Jiao, N. *Angew. Chem.* **2010**, *49*, 6174.

(8) Ahmad, R. K.; Faure, D.; Goddard, P.; Oda, R.; Bassani, D. M. *Org. Biomol. Chem.* **2009**, *7*, 3173.

(9) Nuñez, J. E.; Nataranjan, A.; Khan, S. I.; Garcia-Garibay, M. A. *Org. Lett.* **2007**, *9*, 3559.

(10) (a) Dance, I. *Mol. Cryst. Liq. Cryst.* **2005**, *440*, 265. (b) Stopin, A.; Garcia-Garibay, M. A. *Crys. Growth. Des.* **2012**, *12*, 3792.

(11) (a) Lebedeva, N. V.; Tarasov, V. F.; M. J. E. Resendiz, M. J. E.; Garcia-Garibay, M. A.; White, R. C.; Forbes, M. D. E. *J. Am. Chem. Soc.* **2010**, *132*, 82. (b) Chin, K. K.; Natarajan, A.; Gard, M. N.; Campos, L. M.; Johansson, E.; Shepherd, H.; Garcia-Garibay, M. A. *Chem. Commun.* **2007**, *41*, 4266. (c) Veerman, M.; Resendiz, M. J. E.; Garcia-Garibay, M. A. *Org. Lett.* **2006**, *8*, 2615.

(12) Kasai, H.; Nalwa, H. S.; Oikawa, H.; Okada, S.; Matsuda, H.; Minami, N.; Kuakuta, A.; Ono, K.; Mukoh, A.; Nakanishi, H. *Jpn. J. Appl. Phys.* **1992**, *31*, 1132.

(13) West, R. W. *Solid State Chemistry and its Applications*; John Wiley & Sons Ltd: Chichester, United Kingdom, 2003.

(14) (a) Kumar, G. S.; Neckers, D. C. *Chem. Rev.* **1989**, *89*, 1915. (b) Bandara, H. M.; Burdette, S. C. *Chem. Soc. Rev.* **2012**, *41*, 1809.

(15) Hoatson, G. L.; Vold, R. L. *NMR: Basic Princ. Prog.* **1994**, *32*, 1. (b) Fyfe, C. A. *Solid State NMR for Chemists*; CFC Press: Guelph, Ontario, 1983.

(16) The simulation program NMR-WEBLAB from the Spiess lab is available on the web: Macho, V.; Brombacher, L.; Spiess, H. W. *Appl. Magn. Reson.* **2001**, *20*, 405. (b) The program Express 1.0 from the Vold lab is also available on the web: Vold, R. L.; Hoatson, G. L. *J. Magn. Reson.* **2009**, *198*, 57.

(17) (a) Marahatta, A. B.; Kanno, M.; Hoki, K.; Setaka, W.; Irle, S.; Kono, H. *J. Phys. Chem. C* **2012**, *116*, 24845. (b) Akimov, A. V.; Mandal, D.; Chernyak, V. Y.; Sinitsyn, N. A. *J. Chem. Phys.* **2013**, *138*, 024109. (c) Akimov, A. V.; Kolomeisky, A. B. *J. Phys. Chem. C* **2011**, *115*, 13584.

(18) Simulations were performed using NMR-WEBLAB from the Spiess lab.

(19) O'Brien, Z. J.; Karlen, S. D.; Khan, S.; Garcia-Garibay, M. A. *J. Org. Chem.* **2010**, *75*, 2482.